Boundary-Layer Meteorol
DOI 10.1007/s10546-012-9723-8

ARTICLE

Observations of Diurnal Cycles Over a West African Meridional Transect: Pre-Monsoon and Full-Monsoon Seasons

Amanda Gounou · Françoise Guichard · Fleur Couvreux

Received: 23 September 2011 / Accepted: 28 March 2012

Abstract We document and characterize the climatology of the diurnal cycles encountered along a West African transect during the pre-monsoon and full-monsoon periods. The meridional gradient in low-level properties is fundamental for the monsoon dynamics and here, for the first time, it is studied based on a large set of observations from the African Monsoon Multidisciplinary Analysis (AMMA) campaign. A detailed analysis of surface energy budget, boundary-layer structures and cloud occurrence is carried out to investigate the diurnal cycles of the low levels. A relatively weak meridional gradient of net radiation is observed during the pre-monsoon period, and a large gradient in sensible heat flux is found over the transect with values increasing from south to north. This, as well as the boundary-layer structures, partly explains the large contrasts in the diurnal amplitude of potential temperature and specific humidity along the transect. During the monsoon period, the atmospheric regimes drastically change involving strong interactions between the surface, atmosphere and clouds. The maximum in net radiation is shifted northwards, towards the Sahel, which potentially has a significant impact on the monsoon circulation. The sensible heat flux is considerably reduced and the diurnal amplitude is strongly damped, while the daytime boundary-layer growth decreases significantly in the Sahel related to changes in the balance of boundary-layer processes. These results highlight the contrasted diurnal cycle regimes encountered over West Africa under dry, moist and wet conditions. They provide observationally-based diagnostics to investigate the ability of models to handle the representation of the diurnal cycle over land.

Keywords The AMMA campaign · Boundary layer · Diurnal cycle · Surface–atmosphere interactions · Surface energy budget · West African monsoon

A. Gounou (✉) · F. Guichard · F. Couvreux
CNRM-GAME (Centre National de Recherches Météorologiques), CNRS and Météo-France,
42 Avenue G. Coriolis, 31057 Toulouse, France
e-mail: amanda.gounou@cnrm.meteo.fr

Published online: 26 April 2012

1 Introduction

West Africa is a region in the Tropics that is very sensitive to climatic variability. Strong droughts have raised concerns about our knowledge of the system and predictability (Nicholson 1980). This region exhibits three main zonal climatic zones: Guinean, Sudanian and Sahelian regions (White 1983). This distribution is linked to annual rainfall decreasing from the Equator towards the sub-Tropics (see Fig. 1), with a remarkable zonal symmetry in the precipitation amount and in other meteorological parameters (Janicot et al. 2008).

During the boreal summer, the northward migration of the maximum of insolation generates the inland propagation of a cool and moist flow from the Guinean region towards the Sahel, also called the monsoonal flow. Its northern extension is termed the inter-tropical discontinuity. After a moistening phase, the atmospheric regime changes abruptly due to the northward shift of the inter-tropical convergence zone from 5°N to 10°N, a phenomenon referred to as the monsoon onset (Sultan and Janicot 2003). The diurnal cycle is an important mode of variability in the Tropics (Hastenrath 1995; Yang and Slingo 2001) and especially of the West African monsoon (Parker et al. 2005), which strongly affects the atmosphere at low levels. A critical factor to consider for the monsoon activity is the meridional gradient of boundary-layer conditions between the land region and the Atlantic ocean (Eltahir and Gong 1996; Peyrille and Lafore 2007), suggesting a need for a better characterization of the boundary layer along the meridional transect.

Due to a lack of observations, there are only a few studies on the diurnal cycles in the low levels of the West African monsoon. The Hapex-Sahel campaign, carried out in 1992, provided the first observations on the boundary-layer developments in the Sahel (Goutorbe et al. 1994). Radiosoundings launched during the post-onset period and the retreat of the monsoon revealed changes in boundary-layer behaviour (Wai et al. 1997), but these were limited to a specific site and period of the year. Parker et al. (2005) studied the strong diurnal cycle of the low-level atmospheric dynamics based on JET2000 observations and ECMWF analyses. They found a nocturnal acceleration of the monsoonal flow in the atmospheric low levels at night in response to the pressure gradient between the Guinean coast and the Saharan heat low, which brings moisture inland and affects properties at low levels. Conversely, during daytime, convective boundary-layer development inhibits the northward progression of the monsoonal flow due to turbulent mixing.

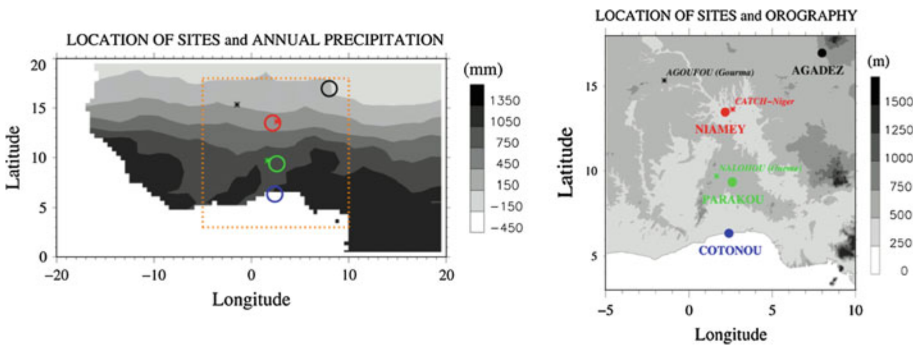

Fig. 1 Location of observation sites plotted over mean annual precipitation from 2005 to 2008 GPCP data (*left plot*); radiosounding stations are indicated using *large circles* at Cotonou (*blue*), Parakou (*green*), Niamey (*red*) and Agadez (*black*), the surface flux stations are represented with *coloured stars*. A zoomed view of the domain is plotted over orography (*right plot*)

During the African Monsoon Multidisciplinary Analysis (AMMA) program (Redelsperger et al. 2006) a large observing campaign was carried out and was designed in order to sample the characteristics along the meridional transect (Lebel et al. 2010), as the monsoon exhibits a remarkable zonal symmetry and a strong meridional climatological gradient (Lebel et al. 2003). The first results show that the nocturnal monsoonal flow acceleration is often associated with a nocturnal low-level jet (Lothon et al. 2008; Abdou et al. 2010; and Bain et al. 2010) in the Sahel. A maximum in the nocturnal wind speeds is typically found at about 0500–0600 UTC. Associated with this acceleration in the monsoonal flow, a strong moistening/cooling of the low levels is observed before the monsoon onset. The water vapour is then redistributed vertically during daytime due to turbulent mixing within the convective boundary layer. Convection also exhibits a strong diurnal cycle with a maximum in convective initiation in the afternoon and a convective activity at night (Mathon et al. 2002; Gounou 2011) that is directly linked to the diurnal cycles of the stability in the atmospheric low levels (Guichard et al. 2008; Kohler et al. 2010). Several important features of the diurnal cycle are typically not well captured by numerical models (Yang and Slingo 2001; Svensson et al. 2011), where simulations are known to develop drifts within one single 24-h period (Betts and Jakob 2002; Guichard et al. 2004; Hourdin et al. 2010). Thorncroft et al. (2003) showed a link between the biases in boundary-layer properties and the representation of the African easterly jet, which is a major feature of monsoon dynamics. Therefore, obtaining a better understanding of the diurnal cycles of dynamic and thermodynamic processes appears also as an important step for improving the understanding and predictability of the West African monsoon system at large scale.

In this study, for the first time, the diurnal cycles in the atmospheric low levels are documented and quantified along the meridional transect with ground-based data and soundings. Indeed, the AMMA campaign provided observations to do this at two key stages of the monsoon: in June before the onset and in August during the core of the monsoon. The aim of this study is to obtain a better understanding of diurnal cycles and the processes controlling them. As a first step towards this goal, the observed diurnal cycles are characterized and extensively discussed.

The data used herein are described in Sect. 2. In Sect. 3, the results are presented with, in particular, a characterization of the diurnal cycle at the surface as well as a description of convective and nocturnal boundary-layer behaviour observed along the meridional transect. Eventually, in order to present the benefits of such data, a comparison of numerical weather prediction (NWP) models against this dataset is shown in Sect. 3.6. Section 4 provides conclusions and discussions.

2 Data and Method

2.1 Intensive Observing Periods and Their Meteorological Contexts

The data used were collected during the AMMA campaign in 2006. In particular, there were two special observing periods (SOP); one before the monsoon onset (20–29 June 2006) and the other during the full-monsoon period (1–15 August 2006); they are referred to hereafter as SOP-1 and SOP-2. During the month of June, the position of the inter-tropical discontinuity, which corresponds to the boundary between the monsoonal flow and the Harmattan (a dry northerly flow), is located north of Niamey (13.5°N, 2.2°E) and can extend to 19°N. In 2006, the monsoon onset was slightly delayed compared to the climatological date of 24 June: it

Table 1 Geographical characteristics of the measurement sites during SOP-1 and SOP-2 and the list of measurements carried out at each site

Site	Country	Latitude	Longitude	Altitude (m)	Sounding (number per day)	Radiative fluxes	Turbulent fluxes
Agadez	Niger	16°97N	7°99E	501	8	No	–
Agoufou	Mali	15°16N	1°48W	305	–	Yes	–
Niamey	Niger	13°48N	2°17E	222	8	Yes	H, LE
Parakou	Benin	9°36N	2°61E	392	8	Yes	–
Nangatchori	Benin	9°65N	1°73E	397	–	No	–
Nalohou	Benin	9°74N	1°60E	449	–	No	H
Cotonou	Benin	6°52N	2°40E	5	8	Yes	–

H and LE stand respectively for surface sensible and latent heat fluxes

occurred around 10 July (Janicot et al. 2008). During the post-onset period, the inter-tropical discontinuity migrated to the north of Agadez. The rainy zone also migrated and extended from 8°N to 16°N (Sudanian and Sahelian regions) with the most intense precipitation located around 10°N.

The characteristics of the two intensive periods are representative of conditions prevailing prior to the onset and during the full monsoon as attested, for instance, by the similarities between the composite based on longer term periods, which will be presented hereafter. These observing periods were devoted to provide the necessary observations at the surface and in the atmospheric low levels with a high measurement frequency to analyze the diurnal cycles along the climatological transect. In the following, we present the data used to describe and document atmospheric vertical structures, surface characteristics and cloud cover over the meridional transect.

2.2 Vertical Structures

Radiosoundings (RS) were launched every 3 h (at around 0000, 0300, 0600, 0900, 1200, 1500, 1800 and 2100 UTC) during these two intensive periods at six different stations (Parker et al. 2008, see Fig. 1 for location). In this study, we focus on four sites (Agadez, Niamey, Parakou and Cotonou) covering the meridional transect (see Table 1 for site characteristics) with Agadez in the northern Sahel, Niamey in the central Sahel, Parakou in the Soudanian zone and Cotonou on the coast of the Guinean gulf. The sondes measure meteorological properties with a vertical resolution of 10–15 m (cf. Table 2), and during the AMMA campaign, dry-biased RS-80 Vaisala sondes were used at several sites. In the present study, we use data corrected according to the algorithm developed by Nuret et al. (2008). Finally, all soundings have been interpolated on a common grid with a fine vertical resolution of 20 m up to a height of 20 km, in order to allow a direct comparison of the diagnostics among soundings and sites.

First, several diagnostics to detect the convective boundary-layer height have been tested. Depending on the inversion strength, some diagnostics have difficulties in identifying correctly the boundary-layer height. The diagnostic used here is the most effective and detects the top of the mixed layer based on the virtual potential temperature profiles. The method consists in comparing the virtual potential temperature (θ_v) at one level to the average θ_v of the levels

Table 2 List of the instruments and their spatial and temporal resolutions

Instrument	Used measured parameters	Time resolution/range	Spatial resolution/range	Location
Radiosoundings	θ, q_v, wind speed and direction	0000, 0300, 0600, 0900, 1200, 1500, 1800 and 2100 UTC	≈10–15 m/0–20 km	Cotonou, Parakou, Niamey, Agadez
Meteorological station	θ, q_v, wind speed and direction	15 min	–	Cotonou, Parakou, Niamey, Agadez
Ceilometer	Cloud base	15 s	60 m	Niamey, Nangachtori
Turbulent Flux station	Sensible and latent heat fluxes	30 min	–	Niamey, Nalohou
Radiative Flux station	Incoming and outgoing shortwave and longwave radiative fluxes	10–30 min	–	Cotonou, Parakou, Niamey, Agoufou
MSG infrared channel	Brightness temperature	15 min	3 km	–
	Rainfall (RFE2)	1 day	0.1°	–

below, $\overline{\theta_v}$. The boundary-layer height is obtained at the level z where $\theta_v(z) > \overline{\theta_v} + 0.25\,\text{K}$, and the estimates are then checked manually and adjusted when needed.

The thickness of the monsoonal flow is estimated based on wind-profile characteristics as used in the literature (Sultan and Janicot 2003). Both the change in zonal direction as well as the minimum of wind speed are used to locate the top of the monsoonal flow. To detect the existence of a nocturnal jet, the wind speed must be greater than $5\,\text{m}\,\text{s}^{-1}$ and greater than that of the flow above the boundary layer. A nocturnal jet is considered as occurring on a given day if a jet is observed in, at least, two vertical profiles per night.

2.3 Surface Data

Surface measurements were collected at different sites along the transect, most of the time collocated with or close to sounding sites. However, when the measurements were not available, data from sites sampling the same part of the meridional gradient are used when relevant (see Fig. 1 for localization of the measurement sites and Table 2 for instrument details).

Radiative flux measurements at the surface from the IMPETUS network were recorded at Cotonou and Parakou (Fink et al. 2006, http://www.impetus.uni-koeln.de/), and they include upwelling and downwelling shortwave and longwave fluxes measured every 10 min. At Niamey, the atmospheric radiation measurement mobile facility station recorded radiative fluxes with 1-min frequency as well as turbulent fluxes with a 30-min frequency (Miller and Slingo 2007).

There were no turbulent flux measurements available at Cotonou, Parakou and Agadez. However, turbulent and radiative fluxes were recorded at Nalohou and Agoufou. Nalohou is situated in the Ouémé basin, 100 km away from Parakou (see Fig. 1), while Agoufou is located in the Gourma region and is representative of central Sahel around 15°N (Mougin et al. 2009) and therefore is the closest to Agadez in terms of climatology. Fluxes at these sites may be different from those at the sounding sites, however, they are relevant to the surface energy budget along the transect. The simulated fluxes from the ALMIP experiment (Boone et al. 2009) were used when observations at Cotonou were missing. The measurements were all averaged over a 1-h period in order to obtain the same resolution for comparison.

In addition, data from the operational network of surface stations of the World Meteorological Organization, referred to as SYNOP data, were collected at the four main sites (Agadez, Niamey, Parakou and Cotonou) every 15 min. These surface measurements were recorded over several years (in the following 4 years, 2005–2008, have been used) and hence allow the assessment of the climatological representativeness of the intensive observing periods.

2.4 Documentation of Clouds and Convection

Hereafter, information on clouds is used to document the context of the two periods as well as to track further synoptic-scale fluctuations. Brightness temperature measures the thermal emission, and data used here are measurements at 10.8 μm from the Meteosat Second Generation (MSG) satellite available every 15 min with a resolution of $3 \times 3\,\mathrm{km}^2$. The minimum, maximum and average of the brightness temperature computed over a $0.25° \times 0.25°$ zone around the site locations are used to estimate the sub-scale cloud-cover variability. If there is a cloud (and aerosols) free pixel in the selected zone, the maximum temperature can be considered as a good proxy for land surface temperature. The minimum temperature gives information on the highest cloud within the selected zone. The variability of brightness temperature reflects whether the cloud field is homogeneous or heterogeneous within the selected zone. Following Söhne et al. (2008), a threshold of $-40\,°$C is used to flag the development of deep convection. The shallow cumulus and stratocumulus clouds are, however, hard to detect with satellite measurements, as they emit longwave radiation at a temperature close to the surface temperature.

At Nangatchori and Niamey, cloud bases are detected from the ceilometer that uses a vertically pointing laser beam with a vertical resolution of 60 m and a temporal resolution of 1 min. In this study, the data are averaged over 15 min and 120 m in the vertical. Moreover a cloud radar and a lidar operated over Niamey at the Arm Mobile Facility site during the two SOPs. They provide, in particular, information on the cloud cover in the close surrounding of the station (Bouniol et al. 2012).

RainFall Estimation version 2.0 (RFE2) data (Love et al. 2004) are estimates of rainfall retrieved from satellite measurements, where the resolution is $0.1° \times 0.1°$ and the temporal resolution is 1 day. To provide an estimate of rainfall and its variability at the four stations, the average, maximum and minimum values are computed over $0.25° \times 0.25°$ zone around the site locations, consistent with the cloud documentation.

3 Results

The following section presents the analysis of observations made during the two intensive observing periods, SOP-1 and SOP-2. This section focuses on the diurnal cycles observed at the surface and in the atmospheric low levels along the West African meridional transect.

3.1 Cloud Cover and Precipitation

The occurrence of clouds is of primary importance for the atmospheric low levels. Indeed, they directly affect the thermodynamic and energy budgets at the surface, in particular, via their interaction with radiation (solar and terrestrial) and the impact of precipitation on soil properties.

Figure 2a illustrates the synoptic variability of cloudiness and precipitation at the four stations during the SOP-1 period based on MSG satellite measurements. At Cotonou, clouds are frequently observed and deep convection regularly develops as attested by the strong negative peak in brightness temperature accompanied by large quantities of rain. During the month of June, the inter-tropical convergence zone extends meridionally from 2°N to 8°N (including the Guinean and Sudanian regions) (Nicholson and Grist 2003). Westward-propagating convective systems triggered during the afternoon intensify over night and bring significant amount of precipitation (Mathon et al. 2002). The amount of accumulated rain received at Cotonou during SOP-1 is estimated at 47 mm based on RFE2 satellite measurements. Low- and mid-level clouds are also often present with a cloud fraction of 20 % below 2,000 m consistent with zonal averages from Stein et al. (2011) and Bouniol et al. (2012).

At Parakou, during SOP-1, deep convection develops almost every day giving rain at night except during a three-day suppressed period (26–28 June) with a total of 16.1 mm from RFE2 estimates. Figure 3b shows the diurnal composite of cloud base from the Nangatchori ceilometer, near Parakou. Shallow cumulus clouds appear to form easily at the top of the convective mixed layer during daytime as soon as the convective boundary layer (CBL) starts to grow, with a maximum of occurrence between 1000 UTC and 1400 UTC (50 % of occurrence). Between 1600 and 1800 UTC, clouds appear to be less frequent (5–10 % occurrence), which has a noticeable impact on the surface fluxes as shown in the following section.

In contrast, over the Sahelian region, north of the inter-tropical convergence zone, cloudy and moist convection is less frequent. Rare cumulus clouds develop during daytime at the top of the atmospheric boundary layer as can be seen on the composite of cloud base occurrence at Niamey (see Fig. 3a). They form, in general, in the morning between 0600 UTC and 1000 UTC, when the low levels are still humid from the advection of the monsoonal flow and/or latent flux from preceding precipitation. They generate only a small amount of precipitation but are important in the vertical transport of water vapour and play a significant role in the energy budget (Benner and Curry 1998; Betts and Jakob 2002; Couvreux et al. 2012). Mid-level clouds are observed essentially during nighttime (20–40 % occurrence) at an altitude of about 4–6 km, which agrees with Bouniol et al. (2012). High-level cirrus clouds are also often present over the Sahel and affect the surface and the atmospheric low levels via their radiative impacts (Fleming and Cox 1974). At Agadez, the brightness temperature is dominated by the diurnal cycle of surface temperature, meaning that only few sparse and shallow clouds occur. The minimum brightness temperature exhibits negative values related to localized cumulus congestus clouds, giving almost no rain.

After the onset of the monsoon, the inter-tropical convergence zone is centred on 10°N. Deep convection develops more frequently in the Sahelian and Sudanian zones, whereas it is suppressed over the Guinean coast. Figure 2b shows the brightness temperature series and the precipitation for SOP-2. The cloudiness is still important at Cotonou, low-level clouds are often present but deep convection is significantly suppressed, as shown by the absence of strong negative peaks in the brightness temperature time series (only 12 mm of rain is estimated). This period corresponds to the short dry season taking place along the Guinean coast. Deep convection intensifies over the Sudanian and Sahelian regions. At Parakou, mesoscale convective systems frequently occur, bringing over 110 mm of rain during SOP-2. Low-level clouds form in the first 500 m of the troposphere between 0000 and 0800 UTC (20–30 % of occurrence), slightly higher with a greater spread in the vertical as the CBL develops between 0800 UTC and 1800 UTC (see Fig. 3b).

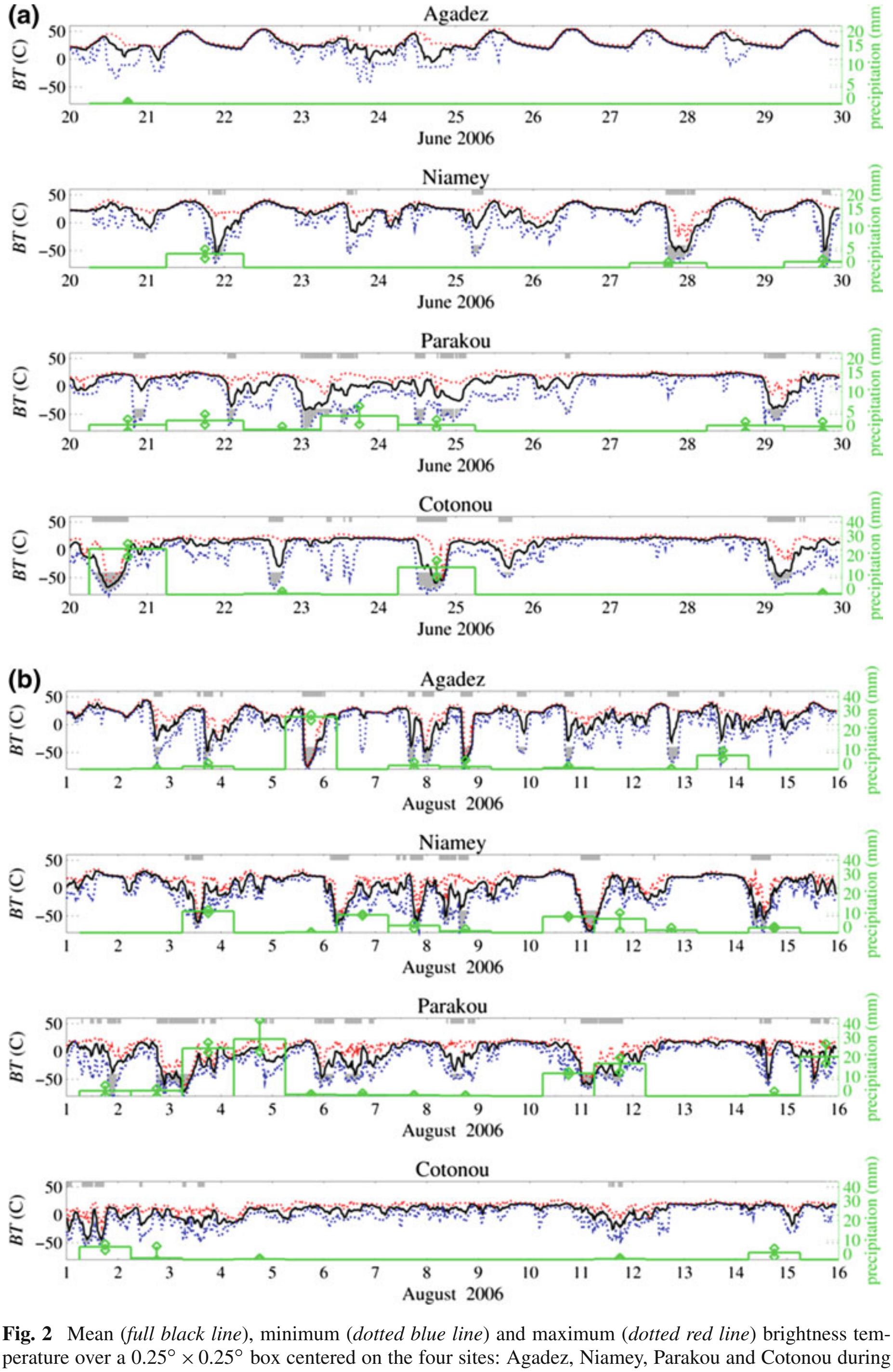

Fig. 2 Mean (*full black line*), minimum (*dotted blue line*) and maximum (*dotted red line*) brightness temperature over a $0.25° \times 0.25°$ box centered on the four sites: Agadez, Niamey, Parakou and Cotonou during SOP-1 (**a**) and SOP-2 (**b**). The *grey shading* represents the development of deep convection using the $-40°$ C threshold. The *green lines* correspond to the mean precipitation from RFE2 estimates over the same *box* and the *bar* indicates the variability inside the *box*

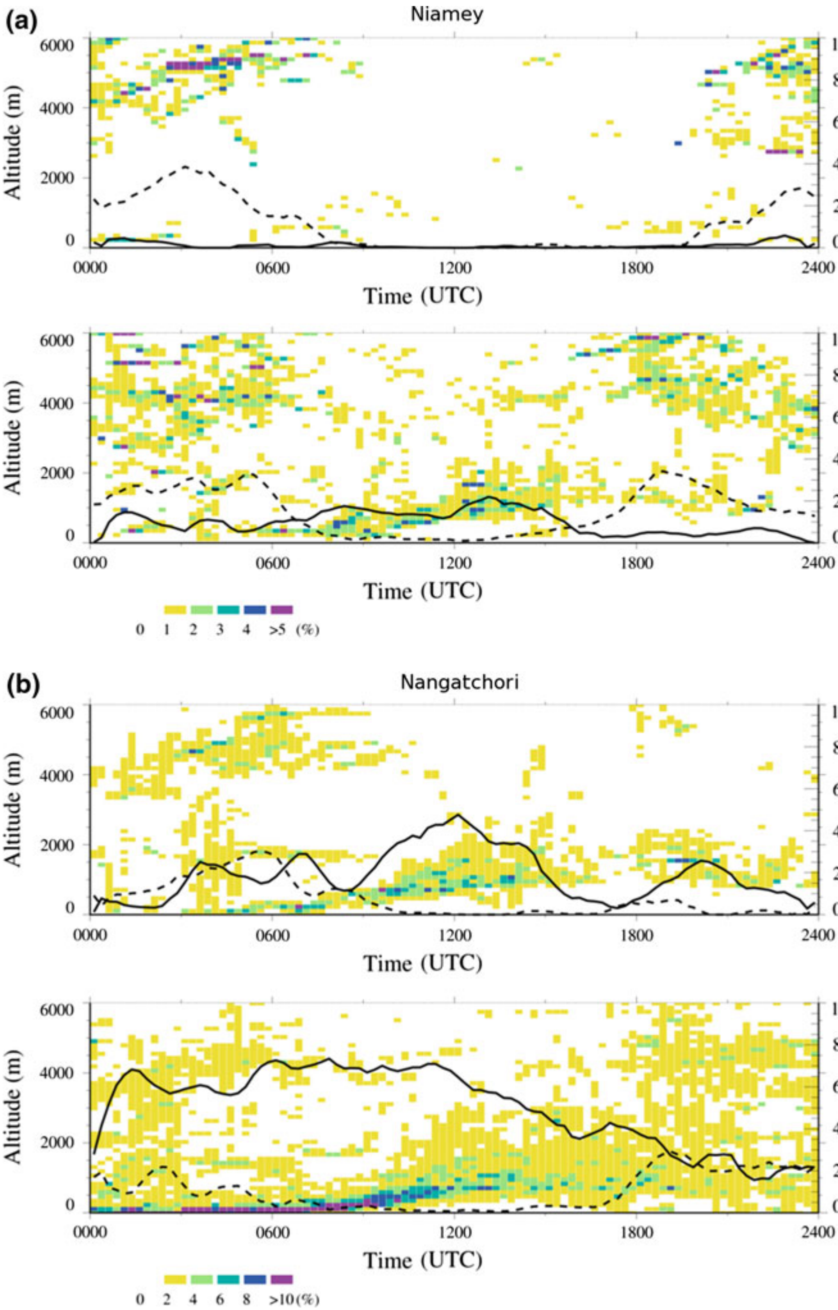

Fig. 3 Composite diurnal cycle of cloud base occurrence (in %) at Niamey (**a**) and at Nangatchori near Parakou (**b**) computed from ceilometer measurements for SOP-1 (*top plot*) and SOP-2 (*bottom plot*). The *colour* of each pixel denotes the percentage of occurrence that a cloud base is detected at a selected height (on a vertical grid of 120-m resolution). Note that the *colour* scales are different for Nangatchori and Niamey. The *black lines* represent the occurrence of cloud base integrated over the vertical in the low levels (0–3,000 m, *full black line*) and mid-levels (3,000–6,000 m, *dashed black line*). This means that there is x % chance of occurrence within a given range of height and time

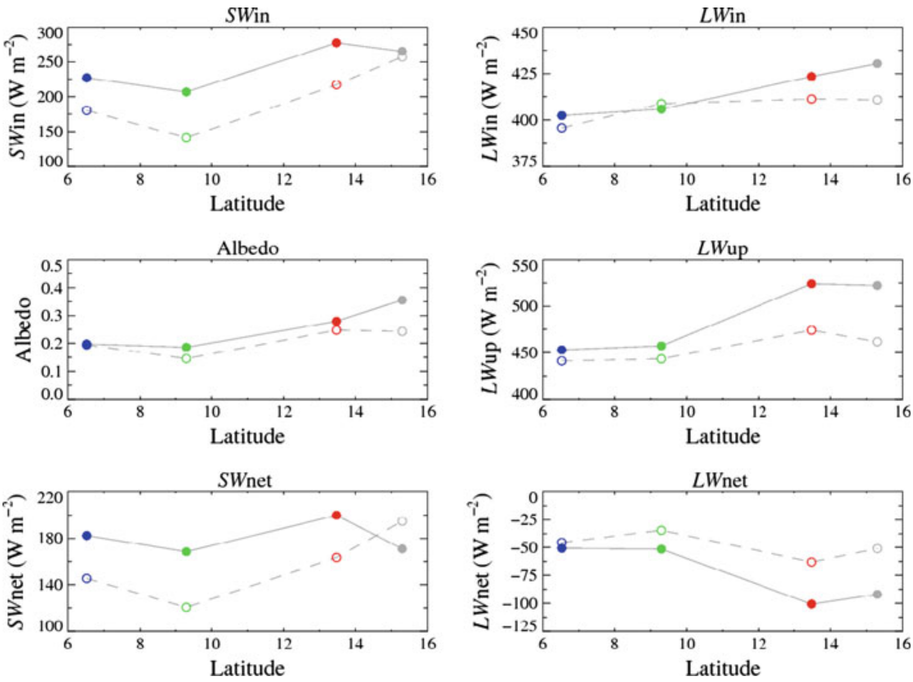

Fig. 4 Daily averaged radiative surface fluxes along the meridional transect: incoming shortwave and longwave radiation (*upper left* and *right plots*), albedo in the visible (*upper left plot*), upwelling longwave radiation (*middle right plot*), net shortwave and longwave fluxes (*bottom plots*) during SOP-1 (*filled circle*) and SOP-2 (*empty circle*, shifted 0.25°N): Cotonou (6°5N, in *dark blue*), Parakou (9°5N, in *green*), Niamey (13°5N, in *red*) and Agoufou (15°N, in *grey*). For Cotonou the longwave fluxes are from the ALMIP data

At Niamey and Agadez, deep convection develops higher than in the Guinean and Sudanian regions but gives less rain (44 mm at Niamey; 54 mm at Agadez). Shallow cumulus clouds form relatively frequently during the daytime in the Sahel as attested by the composite of cloud base from ceilometer measurements at Niamey (20–30 % occurrence see Fig. 3a).

3.2 Energy Budget at the Surface

The energy budget at the surface strongly influences the diurnal cycle of the atmosphere in the low levels and hence it is of primary importance to understand the atmospheric diurnal cycle. In this section, the diurnal variations of radiative and turbulent fluxes are investigated along the meridional transect.

3.2.1 Surface Radiative Fluxes

The daily average of the components of the shortwave and longwave net radiation are plotted in Fig. 4. During SOP-1, the maximum incoming shortwave radiation at the surface (SW_{in}) is found in the Sahel at Niamey ($\approx$280 W m^{-2} on a 24-h average) corresponding to the region combining high incoming solar radiation at the top of the atmosphere and sparse cloud cover as seen previously. At the other stations, SW_{in} is lower due in particular to cloud cover

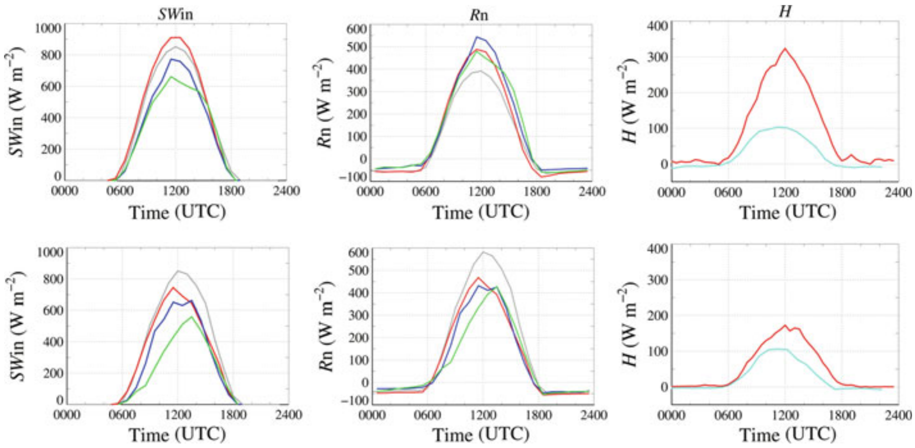

Fig. 5 Composite diurnal cycle of incoming shortwave (*left plots*), net (*middle plots*) radiation and sensible heat (*right plots*) fluxes at the surface during SOP-1 (*upper plots*) and SOP-2 (*lower plots*) along the meridional transect in the observations at Cotonou (6°5N, in *dark blue*), Parakou–Nalohou (9°5N, in *green* and *light blue*), Niamey (13°5N, in *red*), Agoufou (15°N, in *grey full lines*)

(Cotonou: 220 W m^{-2}; Parakou: 200 W m^{-2}). Indeed, at Parakou, frequent cumulus clouds form at the top of the CBL (see Fig. 3) and reduce substantially SW_{in} at the surface, as can be seen in the composite diurnal cycle in Fig. 5. High aerosol concentration also reduces SW_{in}, as in the central Sahel (Agoufou: 260 W m^{-2}). At Niamey and Agoufou, a high surface albedo (0.27–0.35) is responsible for a strong upwelling shortwave radiation (SW_{up}) that contributes to a reduction in the net shortwave radiation. This is partly due to the bright surfaces. The albedo at the other stations is lower (0.15–0.20) due to vegetation (darker) cover (Cotonou, Parakou). The net shortwave radiation, SW_n, is still slightly larger over the central Sahel (Niamey: 200 W m^{-2}) and minimum over the Sudanian region (Parakou: 160 W m^{-2}).

The incoming longwave flux at the surface (LW_{in}) is strongly affected by the temperature stratification and the atmospheric constituents (atmospheric gases, clouds, aerosols). Over the transect, LW_{in} has a mean value between 400 and 430 W m^{-2} with larger values in the north than in the south, even if the precipitable water content and cloud fraction are more important in the south. As one moves to the north, the atmospheric low levels are warmer and therefore emit more radiation in the infrared, even if they have less amounts of water vapour. The diurnal cycle is also stronger in the Sahel ($\Delta LW_{in} \approx 60$–70 W m^{-2}) compared to the Sudanian and Guinean regions ($\Delta LW_{in} \approx 20$–30 W m^{-2}, not shown) linked to diurnal variations of atmospheric properties at low levels. The upwelling longwave radiation (LW_{up}) is higher at Niamey and Agoufou (525 W m^{-2}) compared to Cotonou and Parakou (450–460 W m^{-2}) associated with a higher surface temperature in the Sahel. Eventually, the net longwave radiation, LW_n, corresponding to the LW_{in} minus LW_{up}, is always negative corresponding to an energy loss. This loss is larger in the Sahel (−100 W m^{-2}) than in the southern part of the transect (−50 W m^{-2}), which is of crucial importance at night. Thus, prior to the monsoon onset, the surface radiative budget observed at the Sahelian site is consistent with Charney (1975) who emphasized the role of the Sahara as a maximum of longwave cooling to space in the climate system.

Figure 5 shows a diurnal composite of the surface net radiation ($R_n = LW_n + SW_n$) along the transect. During SOP-1, large SW_{in} is observed over the Sahel but the other components of the radiative budget tend to largely reduce R_n due to a strong albedo and/or large values of

LW_{up}. This leads to only a slight difference along the transect, with a maximum of R_{n} over the Guinean coast and a minimum over the northern Sahel. After sunset, R_{n} becomes negative with the largest negative values found in the early evening (temperature difference between atmosphere and surface being maximum at that time) in the Sahel (Niamey: $-80\,\mathrm{W\,m^{-2}}$).

After the monsoon onset, the incoming shortwave radiation is substantially reduced over the transect (−20 % at Cotonou, −50 % at Parakou, −20 % at Niamey) due to an increase in low-level cloud cover (see Fig. 3). In the northern Sahel (Agoufou), it is only slightly reduced (−3 %) linked to less dense cloud cover and a decrease in mineral aerosol loading (the aerosol optical thickness at 440 nm is on average 0.70 during SOP-1 and 0.55 during SOP-2). Over the Sahel, the albedo decreases (see Fig. 4) associated with a change in surface properties as the vegetation grows. This reduction in albedo, from 0.35 to 0.22, is consistent with the results of Samain et al. (2008) and leads to an increase in SW_{n} in the Sahel (+20 % at Agoufou) whereas the SW_{n} is largely diminished elsewhere due to the reduction in SW_{in}.

The LW_{in} and LW_{up} values substantially lessen over the Sahel towards a behaviour closer to those observed in the south. This is due to lower surface and atmospheric temperatures, as discussed in detail below. The LW_{up} values are more reduced than LW_{in} leading to a smaller negative LW_{n} (reduced loss in energy at the surface compared to the pre-onset period). Over the Guinean and Sudanian regions, only a slight reduction in negative LW_{n} is observed.

In the southern part of the transect, the decrease in R_{n} is mainly attributed to the decrease in SW_{in}. At Niamey, this decrease in SW_{in} is strongly counteracted by a reduction in surface albedo and decrease in LW_{up} (consistent with Ramier et al. 2009). Further north, at Agoufou, the SW_{in} does not decrease compared to that in SOP-1 and the loss of energy by longwave emission is reduced, leading to an augmentation of R_{n} (in agreement with Guichard et al. 2009). Therefore, this meridional gradient in R_{n} changes abruptly from the pre-onset regime to the monsoon regime with a shift in maximum R_{n} from the coast of Guinea towards the central Sahel.

3.2.2 Surface Turbulent Fluxes

The net radiation is partitioned between the ground heat flux, and the sensible and latent heat fluxes. This partitioning is strongly determined by the surface properties (moisture content, soil composition, vegetation cover). Over the West African meridional transect, a gradient is observed in the turbulent flux at the surface as shown in Fig. 5. Before the onset, the maximum of sensible heat flux is observed in the Sahel (Niamey, maximum: $330\,\mathrm{W\,m^{2}}$) associated with dry soils. In the south, the sensible heat flux is much smaller (Nalohou, maximum: $100\,\mathrm{W\,m^{-2}}$) associated with higher soil moisture.

After the onset, a moistening of the soil leads to a decrease in the sensible heat flux in the Sahel (−40 % at Niamey) consistent with previous studies (Dolman et al. 1997; Timouk et al. 2009; Ramier et al. 2009; Kohler et al. 2010). At Nalohou (Parakou), the sensible heat flux remains the same as before the onset, even with a smaller R_{n}. This suggests a smaller latent heat flux or ground heat flux. This involves the evaporative capacity of the atmosphere, which is reduced in moister conditions as shown in van Heerwaarden et al. (2010). The properties of the atmosphere at the surface and in the low levels are hence directly linked to these surface fluxes and are discussed in the following.

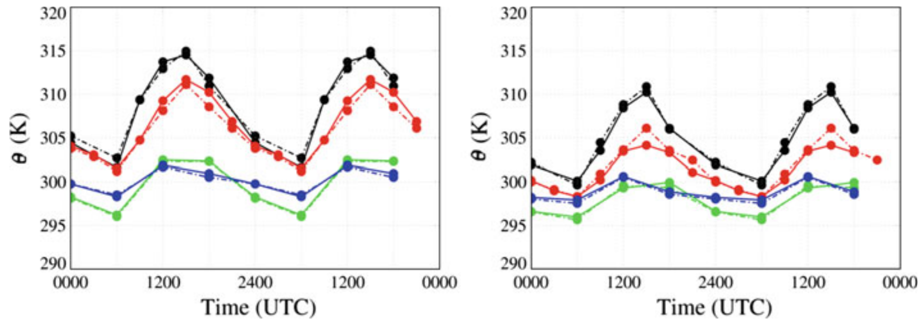

Fig. 6 Composite diurnal cycle of potential temperature at 2 m AGL from the SYNOPs data for the SOP-1 period (*left plot*, *full lines*) and SOP-2 period (*right plot*, *full lines*). The composites over a longer timescale of respectively June and August 2005–2008 are plotted in *dashed-dotted lines*. Note that two composite diurnal cycles are plotted to facilitate the visualization

3.3 Diurnal Cycles in the Atmospheric Low Levels

Figure 6 shows diurnal composites of SYNOP surface potential temperature for the two SOPs compared to the composites for longer term periods (June 2005–2008 and August 2005–2008). It appears that the SOP composites are consistent with the longer time composites. This suggests that the two SOPs are representative of pre-onset and post-onset periods (over the Sahel, SOP-1 is slightly warmer and drier, probably in relation with the late monsoon onset) and SOP-2 is slightly cooler and moister than indicated by the longer time composites.

Compared to the SYNOP data, the radiosoundings are available over a shorter period (only the two SOPs), but they allow us to study the vertical structure of the atmosphere and to assess to what extent SYNOP data (close to the surface) give information on the lower atmospheric levels.

3.3.1 Contrasted Diurnal Cycles Before the Monsoon: Amplitude and Timing

Figure 7 shows the composite diurnal cycles, derived from radiosondes of the thermodynamic (potential temperature (θ) and specific humidity (q_{v})) and dynamic (wind speed (ws)) properties of the atmospheric low levels (averaged over 0–500 m) considering the dry-layer properties, before and after the onset, whereas Fig. 8 presents the cloudy and convective properties of the atmospheric low levels with respectively relative humidity and equivalent potential temperature.

Before the onset of the monsoon, strong meridional contrasts in thermodynamic and dynamical properties are observed. As one moves to the north of the transect, the potential temperature increases (+15 K) and the specific humidity decreases ($-14\,\mathrm{g\,kg^{-1}}$) with the meridional largest differences reached in the late afternoon.

Despite a decrease in R_{n}, there are larger diurnal amplitudes of potential temperature and specific humidity in the northern ($\Delta\theta = 8.1$ K, $\Delta q_{\mathrm{v}} = 4\,\mathrm{g\,kg^{-1}}$ at Niamey) than in the southern part of the transect ($\Delta\theta = 1.4$ K, $\Delta q_{\mathrm{v}} = 1.9\,\mathrm{g\,kg^{-1}}$ at Cotonou). To first order, this is well correlated with the increase in sensible heat flux with latitude. However, other processes and interaction between processes are involved as will be discussed below.

This increase in diurnal amplitude has been previously seen at the surface in the SYNOP data (see Fig. 6), nevertheless, the contrasts in amplitude are less important when considering the low-level values (see Table 3). This is particularly striking at Agadez, where the

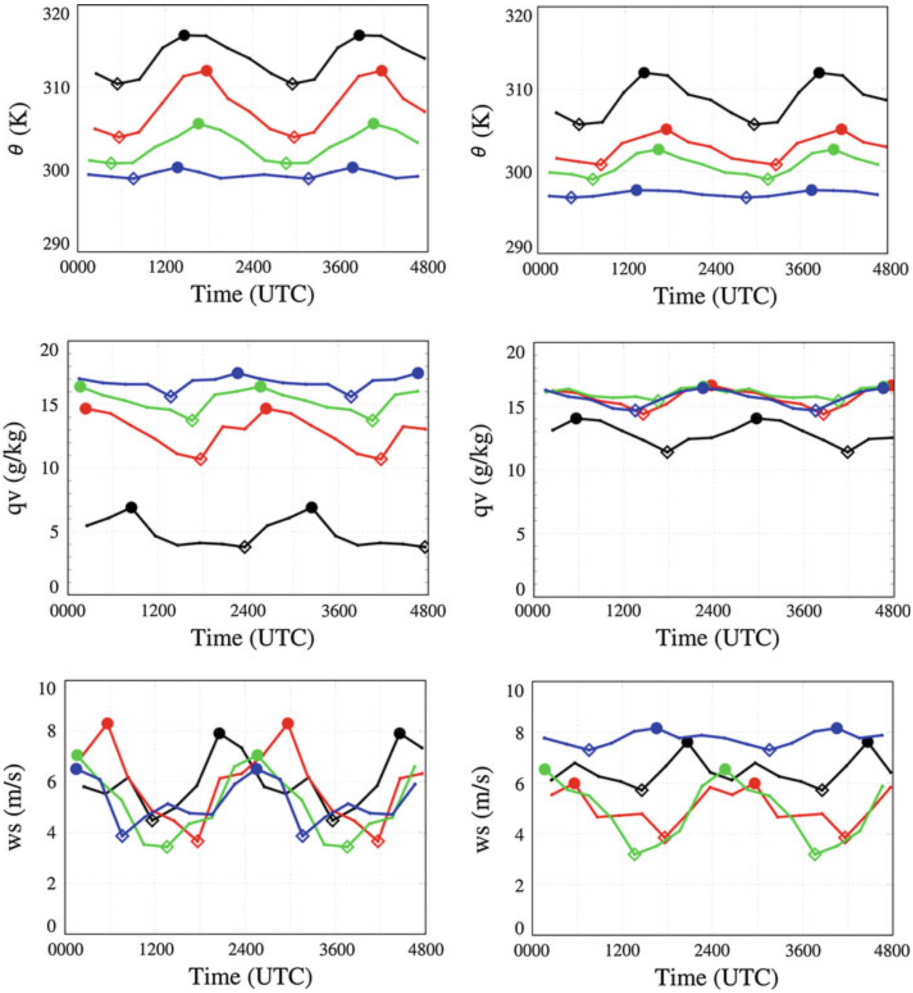

Fig. 7 Composite diurnal cycles of thermodynamic and dynamic properties of the atmospheric low levels (0–500 m) during SOP-1 (*first column*) and SOP-2 (*second column*) at Agadez (in *black*), Niamey (in *red*), Parakou (in *green*) and Cotonou (in *blue*): potential temperature (*top plots*), specific humidity (*middle plots*), wind speed (*bottom plots*) are shown. The *circle* (*diamond shape*) *symbols* indicate the maximum (minimum) values. Note that two composite diurnal cycles are plotted to facilitate the visualization

diurnal amplitude is 12.7 K at 2 m above the ground but only 5.9 K for low-level values. The nighttime surface temperature decreases close to the surface temperatures found at Niamey in Fig. 6. However, when considering the low levels (0–500 m), the cooling is much less intense (Fig. 7). Hence, Agadez exhibits a weaker low-level diurnal cycle of potential temperature than Niamey ($\Delta\theta = 8.1$ K), and this is directly linked to a distinct nocturnal boundary-layer development, which will be explained below. Cotonou has also a low-level diurnal cycle much weaker than at 2 m ($\Delta\theta = 1.4$ K compared to $\Delta\theta = 4$ K at 2 m) associated with a smaller sensible heat flux and a shallow development of the CBL, whose height often does not reach 500 m (see below).

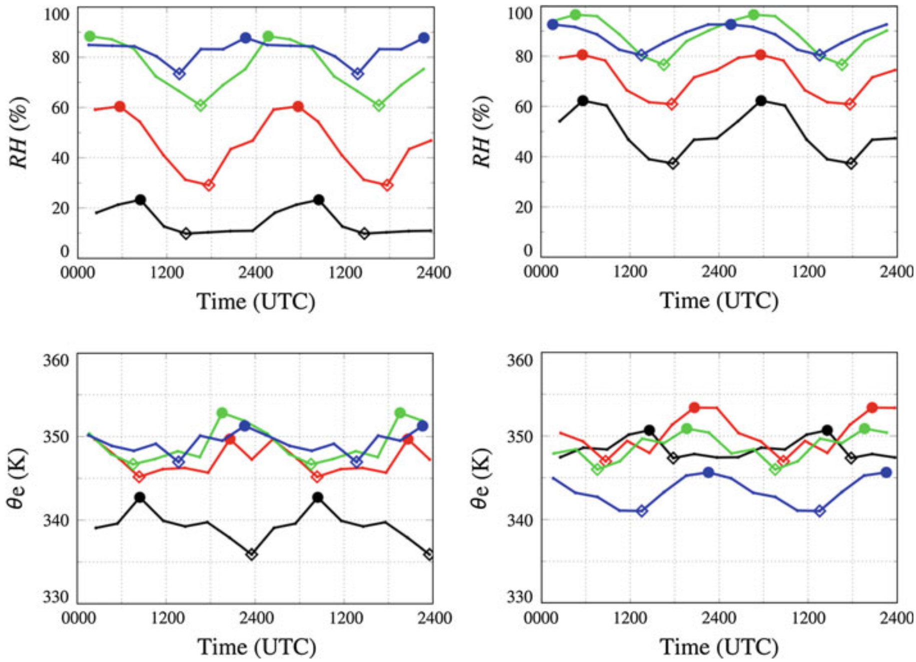

Fig. 8 Composite diurnal cycles of relative humidity (*top plots*) and equivalent potential temperature (*bottom plots*) of the atmospheric low levels (0–500 m) during SOP-1 (*first column*) and SOP-2 (*second column*) at Agadez (in *black*), Niamey (in *red*), Parakou (in *green*) and Cotonou (in *blue*). An offset value of +10 K was added to θ_e at Agadez during SOP-1. Note that the diurnal cycles are plotted over 48 h to facilitate the visualization

Table 3 Diurnal range of potential temperature ($\Delta\theta$), specific humidity (Δq_v), relative humidity (ΔRH) and equivalent potential temperature ($\Delta\theta_e$) at the surface during SOP-1 (bold values) and during SOP-2 (italicized values) computed from between 0 and 500 m from the radiosoundings and at the surface using the SYNOP data (in brackets)

	$\Delta\theta$ (K)		Δq_v (g kg^{-1})		ΔRH (%)		$\Delta\theta_e$ (K)	
Agadez	**5.9 (12.7)**	*6.3 (10.1)*	**3.1 (3.25)**	*2.6 (2.8)*	**13.5 (20.0)**	*24.9 (34.6)*	**6.8 (11.1)**	*3.3 (8.9)*
Niamey	**8.1 (9.3)**	*4.3 (5.8)*	**4.0 (2.77)**	*2.2 (1.4)*	**31.3 (32.7)**	*19.6 (26.9)*	**4.5 (7.2)**	*6.4 (5.2)*
Parakou	**4.8 (6.4)**	*3.6 (4.0)*	**2.7 (1.50)**	*1.1 (1.1)*	**27.6 (24.4)**	*19.9 (14.7)*	**6.2 (12.3)**	*4.9 (8.1)*
Cotonou	**1.4 (4.0)**	*0.9 (2.7)*	**1.9 (0.67)**	*1.8 (0.4)*	**14.3 (16.6)**	*12.2 (12.3)*	**4.3 (7.0)**	*4.6 (4.0)*

An important feature, which has not received much attention in previous studies, is that the timing of the temperature diurnal cycles is also consistently different along the transect. At Agadez, a rapid increase is observed in the morning under cloud-free conditions (linked to properties of the residual layer, see Sect. 3.4), followed by a weaker increase in the afternoon diluted in a deeply developed CBL. The maximum value is reached around 1500 UTC. This behaviour is also observed in the SYNOP data. At Niamey, a more progressive and long-lasting warming occurs; the low-level potential temperature reaches its maximum value at 1800 UTC. The maximum temperatures are reached earlier at Parakou and especially at Cotonou, around midday, linked with the weak development of a CBL and cloud cover. The nightime cooling is strongly affected by the radiative, turbulent and advective processes. R_n is more negative in the Sahel (≈ -100 W m^{-2}) than in the Guinean and Sudanian regions (≈ -50 W m^{-2}), which partly explains the stronger cooling in the north than in the south. The cooling is progressive throughout the night at Agadez, whereas at Niamey there is strong cooling in the early evening and then the temperature decreases progressively. During the nighttime period, the observations available suggest that the monsoonal flow significantly contributes to this early evening cooling at Niamey and Parakou. At Agadez, the nocturnal cooling mainly involves radiative processes and is directly linked to the amount of precipitable water. At Cotonou, the inland progression of monsoonal flow from over the Guinean gulf may not contribute to much cooling.

The day-to-day variability during the period has been quantified by computing the standard deviation for each time in the diurnal cycle (not shown). The maximum variability of θ is found at Niamey and Parakou in the afternoon/early evening, whereas the minimum is observed in the morning. This implies that daytime processes are more sensitive than nighttime processes to synoptic variability. This also distinguishes nighttime to daytime regimes.

The diurnal cycles of specific humidity are also contrasted along the meridional transect. They exhibit a strong daytime drying in the Sahel ($-4\,\mathrm{g\,kg^{-1}}$ at Niamey and $-3\,\mathrm{g\,kg^{-1}}$ at Agadez) due to convective boundary-layer processes (described in more detail below). This drying is very rapid at Agadez and smoother at Niamey, also consistent with the potential temperature variations.

At Cotonou and Parakou, the low levels reveal very weak drying associated with weak convective boundary-layer growth and possibly larger latent heat fluxes related to moist soil. In the evening, a moistening in low levels is observed, which may be associated with evaporation of precipitation (only at Parakou and Cotonou) and monsoonal-flow advection. This moistening process appears to be shifted in time with latitude, which is consistent with the northward progression of the monsoonal flow. The strongest day-to-day variability associated with specific humidity is found at Agadez in the early morning as it lies, in turn, south and north of the inter-tropical discontinuity. The smallest variability is found at Niamey in the afternoon, linked to a steady development of the CBL.

Low-level winds are fundamental to the monsoon circulation and are responsible for the inland propagation of the monsoonal flow. South of the inter-tropical discontinuity (all sites except Agadez), the wind blows from the south-west consistent with the presence of the monsoonal flow (not shown). A slight increase in the westward component of the flow is observed at nighttime at Niamey and Parakou, which is possibly related to the inertial oscillation. At Cotonou, the south-westerly flow observed during daytime veers to the north-west at night, which may be linked to the land-sea contrasts. At Agadez, the airflows most of the time from the north-east corresponding to Harmattan dynamics. The composite of wind speed at the four sites along the transect is shown in Fig. 7 (bottom plots), where the minimum value of wind speed is always found during daytime due to turbulent mixing (about $4\,\mathrm{m\,s^{-1}}$). The maximum wind speed is always reached at night (6–9$\,\mathrm{m\,s^{-1}}$), sometimes associated with a nocturnal jet, in response to a horizontal pressure gradient between the south coast and the Saharian heat low. The timing of this occurrence differs from site to site. At Agadez, this maximum wind speed occurs early in the evening (maybe due to orographic effects and the position of the "heat low") whereas at Niamey and Parakou, it occurs in the early morning (0500–0600 UTC) in agreement with Lothon et al. (2008). This nocturnal acceleration of the horizontal flow allows the northward advection of moister and cooler air at low levels, which has been shown to play an important role in sustaining the monsoonal activity (Parker et al. 2005; Peyrille and Lafore 2007).

The relative humidity at Cotonou is high (70–90 %) readily leading to cloud formation and hence large cloud feedbacks and control on the diurnal temperature range (ΔT). By contrast, at Agadez, the relative humidity is very low (10–20 %), suggesting that the condensation processes have not much control on the diurnal cycle ($\Delta T = 12.7$ K at the surface) and that the radiative imbalance can be greater. Finally, in this region, the equivalent potential temperature in the atmospheric low levels, which is a good proxy for convective available potential energy, e.g. Guichard et al. (2008), displays notable diurnal cycles. Indeed, daytime compensations between specific humidity and potential temperature occur, leading to diurnal cycles of smaller amplitude at Niamey. For example, during daytime, the equivalent potential temperature at low levels does not increase, and even decreases at Agadez, as shown also in the Sahel by Lothon et al. (2011) and Couvreux et al. (2012) for a particular case study, or Guichard et al. (2009) using surface data only. This is a particular behaviour that raises questions regarding the modelling of daytime convection, as many deep convection parameterization schemes are based on convective available potential energy considerations.

3.3.2 A Collapse of the Gradient in Diurnal Cycles During the Monsoon

After the onset of the monsoon, drastic changes of thermodynamic diurnal cycles are observed (see Figs. 6 and 7, right column). First of all, there is a strong mean cooling at all stations especially in the Sahel (at Niamey: −5 K; at Agadez: −4 K) consistent with a decrease in sensible heat flux (Sect. 3.2.2). The daytime increase in potential temperature is reduced especially at Niamey. At 1200 UTC, the maximum temperature is almost already reached (associated with the development of cloudy convection). However, at Agadez the diurnal cycle is mainly shifted towards lower temperatures (−4 K) and the amplitude is slightly increased at low levels (+0.4 K) but reduced at the surface (−1.6 K). The cooling process is more intense at sunset compared to before the onset, consistent with the influence of the monsoonal flow in the northern Sahel. At Cotonou and Parakou, there is a small weakening of the diurnal cycle amplitude (−0.5 K and −1.2 K), as the mean temperature decreases.

During the post-onset period, the inter-tropical discontinuity is always located north of Agadez. The atmosphere is moister at all sites (+7 $\mathrm{g\,kg^{-1}}$ at Agadez, +2 $\mathrm{g\,kg^{-1}}$ at Niamey) except at Cotonou (−1 $\mathrm{g\,kg^{-1}}$). The diurnal cycles of specific humidity are now in phase at Cotonou, Parakou and Niamey. There is a moistening from midday until midnight and then a drying from midnight to midday. At Agadez, the diurnal cycle is different from the other stations; the low levels are drier and nighttime moistening occurs throughout the night, but similar to the diurnal cycle found at Niamey during SOP-1, as discussed in more detail below.

This post-onset period is characterized by a strong mean amplification of south-westerly winds at Cotonou (+2.5 $\mathrm{m\,s^{-1}}$), while its diurnal cycle vanishes suggesting weaker sea-land breeze influences during the post-onset period. At the same time, lighter winds are observed in particular at Niamey at night (−2 $\mathrm{m\,s^{-1}}$) linked to a weakening of nocturnal jet activity. At Agadez, the daytime wind speeds are greater than during the pre-onset period. Overall, the diurnal cycle of the wind speed is weaker, consistent with Parker et al. (2005).

There is also a mean increase in relative humidity over the whole transect (even at Cotonou, despite an observed decrease in specific humidity, highlighting a compensating effect between the temperature and specific humidity). A significant augmentation of equivalent potential temperature is found over the Sahel (+20–25 K at Agadez). A maximum is found

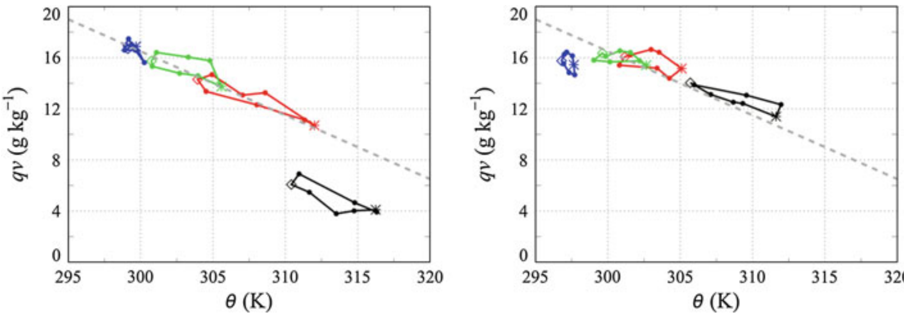

Fig. 9 Composite diurnal cycle of specific humidity as a function of potential temperature in the low levels (0–500 m) at Agadez (*black*), Niamey (*red*), Parakou (*green*) and Cotonou (*blue*) before (*left plot*) and after (*right plot*) the onset of the monsoon computed from the radiosounding data. The *diamond-shaped symbol* represents the 0600 UTC data point and the *star* corresponds to the 1800 UTC radiosounding. The *dotted line* is the line $q_{\mathrm{v}} = -0.5\theta + 165.5$

in the afternoon at Agadez whereas it is found later at night at the three other stations. The equivalent potential temperature substantially decreases at Cotonou (-7 K) associated with the cooling and drying of the atmospheric low levels.

3.3.3 Similarities and Differences Between the Atmospheric Regimes

As seen in the previous section, there are large atmospheric regime changes before and after the onset of the monsoon at each station. However, we find similarities between some pre-onset and post-onset regimes. Figure 9 shows the composite diurnal cycles of specific humidity as a function of potential temperature. A shift towards moister and cooler atmospheric regimes is observed after the onset of the monsoon along with the displacement of the inter-tropical convergence zone. Agadez during SOP-2 presents a diurnal cycle close to the Niamey diurnal cycle during SOP-1 (see also profiles in the Appendix Fig. 13). Slight differences can be noticed in the temperatures that are still higher at Agadez, and the amplitude is smaller. Other similar regimes are observed: Niamey during SOP-2 closely resembles Parakou during the pre-onset period. In turn, Parakou during SOP-2 also exhibits similarities with the atmospheric regime found at Cotonou during the pre-onset period. Similarities are also found in the convective and nocturnal boundary-layer developments, which are discussed below. The diurnal amplitude increases with increasing potential temperature except in limiting conditions as at Agadez. The diurnal cycles of θ and q_{v} are negatively correlated (from cooler-moister to warmer-drier) with similar behaviour except at Cotonou during the monsoon period, where diurnal variations are mostly in humidity.

3.4 Convective Boundary-Layer Growth

The CBL characteristics are important to understand the low-level evolution as the air is mixed throughout the boundary layer and hence affects the low levels via turbulent processes (Stull 1988). The notion of the boundary-layer height is also important in terms of atmospheric stability and cloudy convection. Figure 10 shows the temporal evolution of the CBL height estimated from radiosounding measurements. Before the beginning of the monsoon activity over the Sahel, the depth of the CBL significantly increases with latitude. It is relatively shallow at Cotonou (about 200–400 m) and Parakou (about 1,000–1,500 m), but particularly deep in the northern Sahel, at Agadez (up to 5500 m) and at Niamey to a lesser

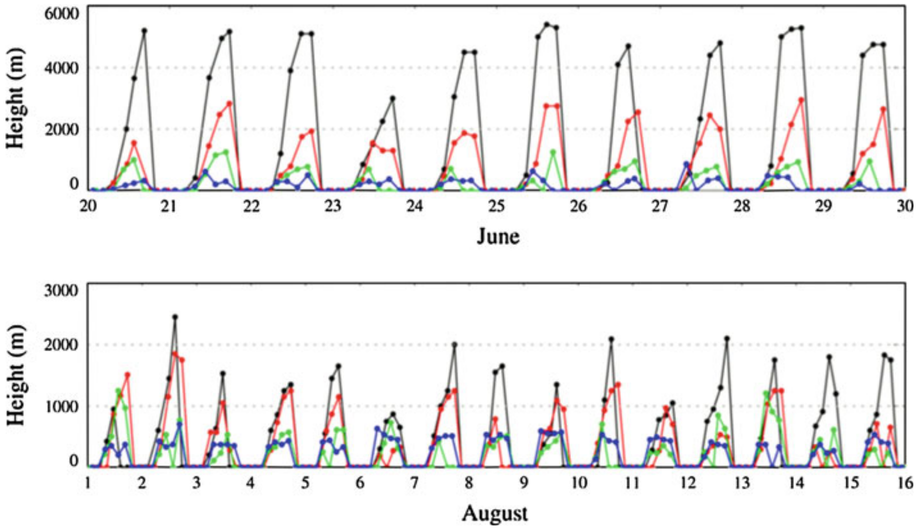

Fig. 10 Temporal evolution of boundary-layer height estimated from radiosoundings at Agadez (*black lines*), Niamey (*red lines*), Parakou (*green lines*) and Cotonou (*blue lines*) during SOP-1 (*top plot*) and SOP-2 (*bottom plot*)

extent (up to 3,000 m). The CBL reaches a maximum height between 1500 UTC and 1700 UTC, though the timing of boundary-layer growth is different from one site to another. The growth of the boundary layer is strongly dependent on the sensible heat flux, the stability of the free atmosphere and the entrainment processes to a lesser extent, which will depend on the different locations along the transect as follows.

At Agadez, after having overcome a strong but very thin nocturnal inversion, the CBL grows rapidly within a persistent layer characterized by weak stability, referred to as the Saharian atmospheric layer (Cuesta et al. 2008). At about 1500 UTC, the CBL has almost reached its greatest depth on most days. Associated with the rapid and large development of the boundary layer, a strong drying of the atmosphere (1 g $kg^{-1}hr^{-1}$) is observed, as shown in Fig. 7, and due to dry-air entrainment. Also due to this rapid development, the warming of the CBL is large in the morning but decreases rapidly as the CBL evolves within the Saharian atmospheric layer (no entrainment of warmer air into the CBL) and a decrease of sensible heat-flux divergence over a deep layer. At midday, a large day-to-day variability is observed in the boundary-layer height (2,000–5,000 m) while very weak variability is observed in the late afternoon, the inversion at the top of the Saharian atmospheric layer preventing further growth of the CBL. On one occasion only (23 June) does the boundary layer remain relatively shallow (3,000 m), linked to the presence of low-level cumulus clouds (Fig. 2) that reduce the incoming shortwave radiation (and hence sensible heat flux at the ground) preventing strong development of the dry boundary layer. The afternoon day-to-day fluctuations may be also closely linked to the mineral aerosol concentrations that largely vary at the synoptic scale (Kocha et al. 2012).

At other stations, the development is dissimilar, where the CBL grows within a more stable environment. At Niamey, the sensible heat flux is larger than at Agadez in June (see Fig. 5) as the soil remains dry and R_n is larger. However, the atmosphere is cooler and more stable than at Agadez. The boundary layer therefore develops more regularly throughout the day, entraining drier and warmer air. Hence, the atmosphere dries and warms all day long with only few cumulus clouds developing at the top of the CBL (see Fig. 3). At Niamey, strong wind shear is found at the top of the CBL due to the presence of the African easterly jet that amplifies the entrainment rate (Canut et al. 2010). The advection from the monsoonal flow, which cool the low levels, also play a role in the development of the CBL. The day-to-day variability in boundary-layer height is at its maximum at the end of the afternoon with values ranging from 1,500 to 3,000 m.

At Parakou, cumulus clouds frequently form at the top of the CBL early in the day (on average around 1000 UTC, Fig. 3a), resulting in the stabilizing of the atmospheric θ profile and also diminishing SW_{in} at the surface. The mixed-layer growth ceases by early afternoon. However, a drying and warming of the atmosphere is still observed until 1800 UTC suggesting that dry air from the free troposphere is still entrained into the boundary layer. At Cotonou, located close to the Guinean gulf, the atmospheric boundary layer is largely influenced by the advection of low-level air originating from the Guinean gulf. Therefore, the boundary-layer properties are only weakly affected by the local land surface, a land surface that is characterized by high soil moisture and low sensible heat flux (see Sect. 3.2). The CBL remains shallow in association with this small sensible heat flux, stable atmospheric profile and the presence of clouds. A moistening of the boundary layer is observed in the morning associated with surface evaporation that is larger than the water vapour flux associated with the entrainment of dry air from the free troposphere. Inversely, at midday, a slight drying is found suggesting that the surface evaporation is smaller than the water vapor flux associated with dry air entrainment.

During the core of the monsoon, the development of the CBL is drastically changed in the Sahel. The CBL grows less, in particular at Agadez, where it reaches a maximum height of <2,000 m instead of 5,000 m in June. The CBL is colder at all sites and moister, except at Cotonou where it is drier. At Agadez, the atmospheric profiles are now influenced by the monsoonal flow, with the consequence of cooling the atmospheric low levels and stabilizing the morning vertical profile over a deeper layer (see Appendix Fig. 13). Moreover, the sensible heat flux is significantly smaller due to soil moisture (see Fig. 5) and, at higher levels, the atmosphere is warmer (more stable) than before the onset. These changes in the atmospheric stability and in the surface sensible heat fluxes contribute to a decrease in the CBL growth. Another limiting factor in the CBL growth is the moistening of the low levels. Indeed, during the full monsoon, the lifting condensation level is lower and often coincides with the top of the mixed layer. Therefore, the low-level moistening restrains the depth over which dry convective processes can develop, or in other words the CBL growth. Similar changes occur at Niamey where the top of the mixed layer only reaches 1,000–1,500 m instead of 2,000 m during the pre-onset period. At Parakou, the CBL develops only slightly less compared to the pre-onset period (the CBL top reaches 500 m on average). Daytime drying is weaker associated with less dry-air entrainment.

As in Marht (1991), there are two different prototypes of boundary layer: one that is dominated by dry-air entrainment as observed at Agadez during the monsoon period and at Niamey during the pre-onset period. The other prototype is observed at other sites during the monsoon season where there is competition between moistening from surface fluxes and drying from entrainment at the top of the CBL.

3.5 Nocturnal Boundary Layer

The contrasted daytime boundary layers discussed above are coupled to very distinct nocturnal boundary layers. Their main features are presented below, in terms of depth, nighttime evolution and jet occurrence.

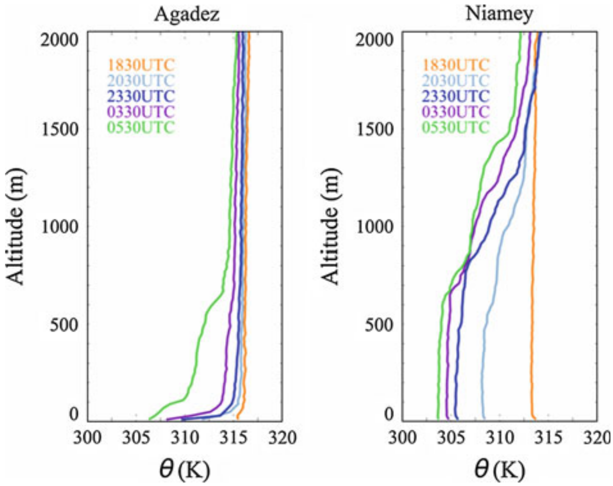

Fig. 11 Nocturnal profiles of potential temperature at Agadez (*left plot*) and Niamey (*right plot*) between the 26 June 2006 at 1830 UTC and 27 June 2006 at 0530 UTC from radiosounding measurements

Before the onset of the monsoon, there is a thin (<100 m) and very stratified nocturnal boundary layer at Agadez under dry conditions, associated with large radiative cooling, as illustrated in Fig. 11 (see also composite profiles in the Appendix Fig. 13). At Agadez, the net radiation at the surface at night is largely negative, as seen in Fig. 5, due in particular to the dryness of the atmosphere. A clear correlation is found between precipitable water in the atmosphere and nocturnal cooling at the surface (not shown). The drier the atmosphere, the more negative is the net longwave radiative flux at the surface. The whole atmospheric column is also cooled down by several K. In this stable boundary layer, the wind becomes lighter compared to the free troposphere (see Appendix Fig. 13); a nocturnal jet sometimes forms at the top of this layer, with a frequency occurrence of 35 % during SOP-1, which does not appear in the composite profiles.

At Niamey, the nocturnal boundary layer is usually much deeper than at Agadez (200–800 m) and is associated with a greater level of turbulence. The temperature profile is significantly less stable than at Agadez. Sometimes, a remarkable cool nocturnal layer with neutral stability is observed at Niamey. This thermodynamic structure is linked to the monsoonal flow as well as the dynamics of the nocturnal jet that creates turbulence. Indeed, a nocturnal jet often forms at Niamey during SOP-1 (frequency of occurrence of 60 %). For illustration purpose, nocturnal profiles of potential temperature for the night of 26–27 June are shown for Agadez and Niamey in Fig. 11, illustrating the contrasted boundary layer encountered at Agadez and Niamey. At Parakou, the nocturnal boundary layer is more stratified than at Niamey.

At Cotonou, before and after the onset of the monsoon, the vertical profiles do not exhibit much of a change in lapse rate, which makes it difficult to detect the nocturnal boundary-layer height. The nocturnal boundary layer is weakly stratified and remains shallow (about 100 m deep) with almost no nocturnal variation in the profiles at low levels. More variability occurs at higher altitudes, above the monsoonal flow. The monsoonal-flow thickness reaches altitudes between 1,000 and 2,000 m without an evident meridional gradient in thickness during the pre-onset period according to sounding data at the four sites. It does not exhibit a clear diurnal cycle either and its thickness remains relatively constant

Table 4 Characteristics of the low-level nocturnal jet during SOP-1 and SOP-2: frequency of occurrence, averaged maximum speed and altitude

	SOP-1			SOP-2		
	Freq (%)	Speed (m s^{-1})	Altitude (m)	Freq (%)	Speed (m s^{-1})	Altitude (m)
Agadez	35	9.9 (5.9–15.2)	230 (110–370)	80	9.4 (5.2–17.0)	260 (130–670)
Niamey	60	10.9 (5.1–19.0)	320 (90–670)	85	8.5 (5.2–15.6)	360 (170–730)
Parakou	55	8.6 (5.3–19.3)	300 (130–590)	50	8.1 (6.0–12.0)	255 (110–430)

The minimum and maximum values are indicated in brackets

throughout the night. During the monsoon, the flow is deeper close to the coast, at Cotonou and Parakou, possibly linked to the absence of the African easterly jet that has migrated to the north.

Nocturnal low-level jets are observed along the transect except at Cotonou; their characteristics are listed in Table 4. The low-level nocturnal jet forms at an altitude of 100 m to 700 m, with a mean altitude of 230 m at Agadez, 320 m at Niamey and 300 m at Parakou. The average jet speed is greater at Niamey (10.9 m s^{-1}) than at Parakou (8.6 m s^{-1}) and Agadez (9.9 m s^{-1}). Nocturnal low-level jets are also more frequently observed at Niamey than at Parakou and Agadez. At Parakou and Niamey, the nocturnal-jet flow is from the south-west, whereas at Agadez it is from the north-east. Hence, at Niamey and Parakou, south of the inter-tropical discontinuity, nocturnal low-level jets are associated with the northward transport of moisture, which has a large impact on the convective activity, and helps the northward propagation of the inter-tropical discontinuity. North of the inter-tropical discontinuity, the nocturnal jet accelerates the Harmattan flow, which is dry and warm. The nocturnal jet appears to have a large impact on the low-level stability at Niamey. Enhanced turbulence leads to a deeper nocturnal layer, and is associated with less nocturnal cooling at the surface via the mixing down of warmer air, but larger cooling aloft. Furthermore, the advected flow is also typically cool and moist. These nocturnal processes influence the growth of the following CBL, which is moister but shallower. At Agadez, the nocturnal low-level jet forms above the nocturnal boundary layer and does not contribute to the mixing down of warmer air. Therefore, strong cooling is observed at the surface and not in the lower levels. In the morning, thermals forming in the CBL transport momentum downwards from the nocturnal jet and hence a maximum in surface wind speed is observed. This mechanism is important for dust uplift into the boundary layer.

During the full-monsoon period, nocturnal wind speeds lessen at Parakou and Niamey but increase at Agadez and Cotonou, and the occurrence of nocturnal jets diminishes at Parakou possibly due to the effect of deep convection. However, they are more frequent at Niamey and Agadez. During this period, all nocturnal jets have the effect of accelerating the monsoonal flow. However, the meridional gradients of water vapour between the Guinean coast and the southern Sahel are much weaker than during the pre-onset period. Therefore, nocturnal jets only contribute weakly to the moistening of low levels, except at Agadez, where the influence of advection is still large.

3.6 Comparison with Numerical Weather Prediction Models

At this stage, doubts arise regarding the accuracy of the modelling of such consistently distinct boundary layers. This is briefly discussed here using results from two NWP forecasts:

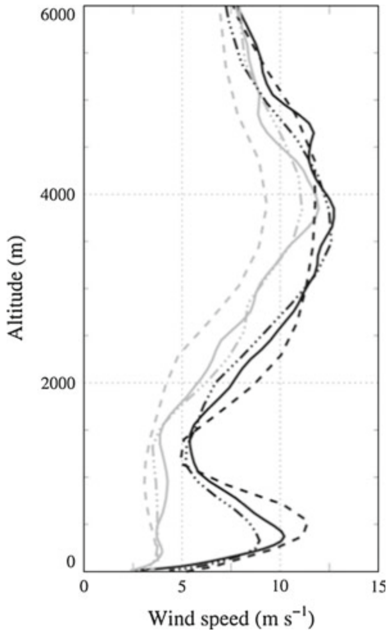

Fig. 12 Composite vertical profiles of wind speed at 0600 UTC (*black lines*) and 1800 UTC (*grey lines*) at Niamey during SOP-1 in the radiosoundings (*full lines*), in the forecast from ARPEGE analysis (*dashed lines*) and in the forecast from the ECMWF re-analysis (*dashed-dotted lines*)

the ECMWF AMMA-re-analysis (Agusti-Panareda et al. 2010) and the ARPEGE operational model (Karbou et al. 2010).

As an example, Fig. 12 compares the profiles of wind speed at Niamey during SOP-1 in these two forecasts with radiosoundings, and are typical of what was observed at other Sahelian sites. Note that 0000 UTC soundings at this site were assimilated in the analyses on which the forecasts are based. It appears that these models have difficulties in simulating the diurnal dynamics and they exhibit various biases. During nighttime, the fine-scale low-level structures are hard to capture. Indeed, the models have difficulties in reproducing the nocturnal inversion that arises from a subtle equilibrium between turbulent, radiative and advective processes. ARPEGE generates an overly strong low-level jet that produces too much turbulence and hence generates thermodynamic profiles that are mixed over too deep a layer (not shown). In contrast, in the ECMWF re-analysis, the nocturnal jet is underestimated and the thermodynamic structure is too stable compared to the observations, as also found by Bain et al. (2010). This may lead to an underestimation of the advection of humidity in the low levels with consequences for the monsoon dynamics. Then, starting from relatively close early-morning thermal structures, the simulated thermodynamic profiles are found to depart more quickly from observations during daytime (compared to nighttime), when the magnitude of the surface heat exchange increases (not shown). This in turn affects the simulated daytime convective activity and clouds.

4 Conclusion and Discussion

This study is based on a unique set of observations that was gathered during the AMMA campaign. It highlights contrasted diurnal cycles in the atmospheric low levels along a meridional transect extending from the Guinean coast (Cotonou) to the northern Sahel (Agadez). The study focuses on the phase preceding the monsoon onset and the well-established phase of the monsoon.

First, an analysis of surface fluxes allows us to characterize and quantify the energy budget at the surface. Before the onset, even in the presence of a strong spatial gradient in incoming shortwave radiation along the transect, there is only a slight meridional decrease in the surface net radiation from the Guinean coast to the Sahel. This compensating effect is linked to larger albedo and longwave cooling in the Sahel. The surface and soil properties play an important role in the meridional variability. The soil moisture strongly modulates the net radiation partitioning into sensible and latent heat fluxes; in the southern part of the transect, low sensible (strong latent) heat fluxes are found, whereas, in the Sahel, the opposite is observed. After the onset, the incoming shortwave radiation is significantly reduced over the southern part of the meridional transect due to an increase in cloud cover, but not in the central and northern Sahel (due to a lesser increase in cloud cover and a decrease of aerosol loading). However, in the southern part, the surface net radiation is only slightly modified due in particular to a decrease in upwelling shortwave and longwave radiative fluxes; this is particularly true in the southern Sahel (Niamey). The meridional gradient of net radiation is changed compared to the pre-onset period, with a maximum found in the Sahel, with major impacts on the monsoon circulation as stressed by Eltahir and Gong (1996) and Chou and Neelin (2003). The turbulent fluxes are drastically changed over the Sahel, with a large reduction in sensible heat flux due to a moistening of the soil by precipitation.

Then, the atmospheric diurnal cycles at the surface and in the low levels are characterized and quantified using SYNOP data and radiosoundings respectively. According to the latitude and season, different amplitudes, phases and structures of the diurnal cycle of temperature and humidity are observed. They are associated with distinct balances of physical and dynamic processes. Overall, the amplitude of the surface diurnal cycle increases with increasing mean temperature observed in drier conditions. However, the low-level diurnal cycle exhibits slightly different behaviour, suggesting that one should be cautious when using SYNOP data to infer characteristics of the low-level diurnal cycle. For instance, at Agadez during the pre-onset period, the amplitude of the low-level potential temperature diurnal cycle is smaller than at Niamey, which is directly linked to the nighttime boundary-layer vertical structure (at Agadez, there is a strong nocturnal cooling but only within a very thin surface layer). Conversely, these findings also point to the fact that the conditions prevailing at the surface are largely influenced by processes taking place within a very shallow nocturnal layer under the driest encountered conditions, when the surface and lower atmosphere are less thermally coupled (Betts 2006).

The radiosounding data allow us to characterize the vertical structures of the convective and nocturnal boundary layers. Diagnostics on the CBL (i.e. height, atmospheric stability, monsoonal-flow thickness) highlight the large contrasts in the vertical structures along the transect before the onset of the monsoon. A deep CBL develops in the northern Sahel (more than 5 km deep) but remains very shallow at the Guinean coast (<500 m). These developments largely influence the properties of the atmospheric low levels by constraining the warming and drying rates as well as the development of cloudy convection. After the monsoonal onset, drastic changes in the dynamic and thermodynamic diurnal cycles are observed: in the northern Sahel, the CBL height significantly decreases (1.5–2 km deep), and the diurnal cycles along the transect become closer together in terms of timing and amplitude.

The nocturnal boundary layer is also characterized using the diagnostics of height, stability, nocturnal jet, monsoonal-flow thickness. Different behaviour is observed along the transect, with a very thin and strongly stratified nocturnal layer at Agadez before the onset, whereas a deep and weakly stratified nocturnal boundary layer is observed at Niamey. Nocturnal jets often occur along the transect.

This set of measurements provides information on the varied boundary-layer regimes found over land from the wet tropics to the sub tropics of West Africa. A stratification of the low levels according to their mean temperature and humidity provides a valuable common framework to interpret these contrasted behaviours; it further points to basic features of the lower atmosphere over West Africa, which are related to coupled temperature–humidity fluctuations in space and time.

As briefly discussed, current NWP models should be used with caution regarding their simulation of the lower atmosphere: inaccuracies in daytime surface heat fluxes affect the thermodynamic properties of the simulated CBL while the low-level nocturnal wind and advection are sensitive to the modelling of subtle couplings between surface, turbulence and radiative processes. The results presented here should be useful in model evaluation projects such as the AMMA-Model Intercomparison Project (Hourdin et al. 2010) that already highlighted major issues in the simulation of the West African monsoon in climate models. The identified and quantified vertical structures such as the boundary-layer height, as well as the thermodynamic and dynamics quantification of diurnal regimes, will be valuable to evaluate more fully numerical models along the West African meridional transect. A careful analysis of low-level processes in these models will be possible within the CFMIP project (McAvaney and Le Treut 2003; Williams et al. 2006) as it provides high-frequency detailed model budgets precisely at these locations. More broadly, this study provides observationally-based diagnostics allowing the study of the behaviour of physical parametrizations under highly contrasting continental regimes.

Acknowledgments Based on a French initiative, AMMA was developed by an international scientific group and is currently funded by a large number of agencies, especially from France, the UK, the US and Africa. The authors would like to thank AMMA-Catch, the Centre of Ecology and Hydrology and IMPETUS for the surface data, the ARM Mobile Facility team for measurements at Niamey, and Suzanne Crewell for the ceilometer observations at Djougou. We also would like to thank Florence Favot for the softwave support, Jean-Marcel Piriou, Martin Koehler for providing the NWP model outputs. We are grateful to the reviewers for their valuable comments on the manuscript and also to Matt Freer for English corrections

Appendix

See Fig. 13.

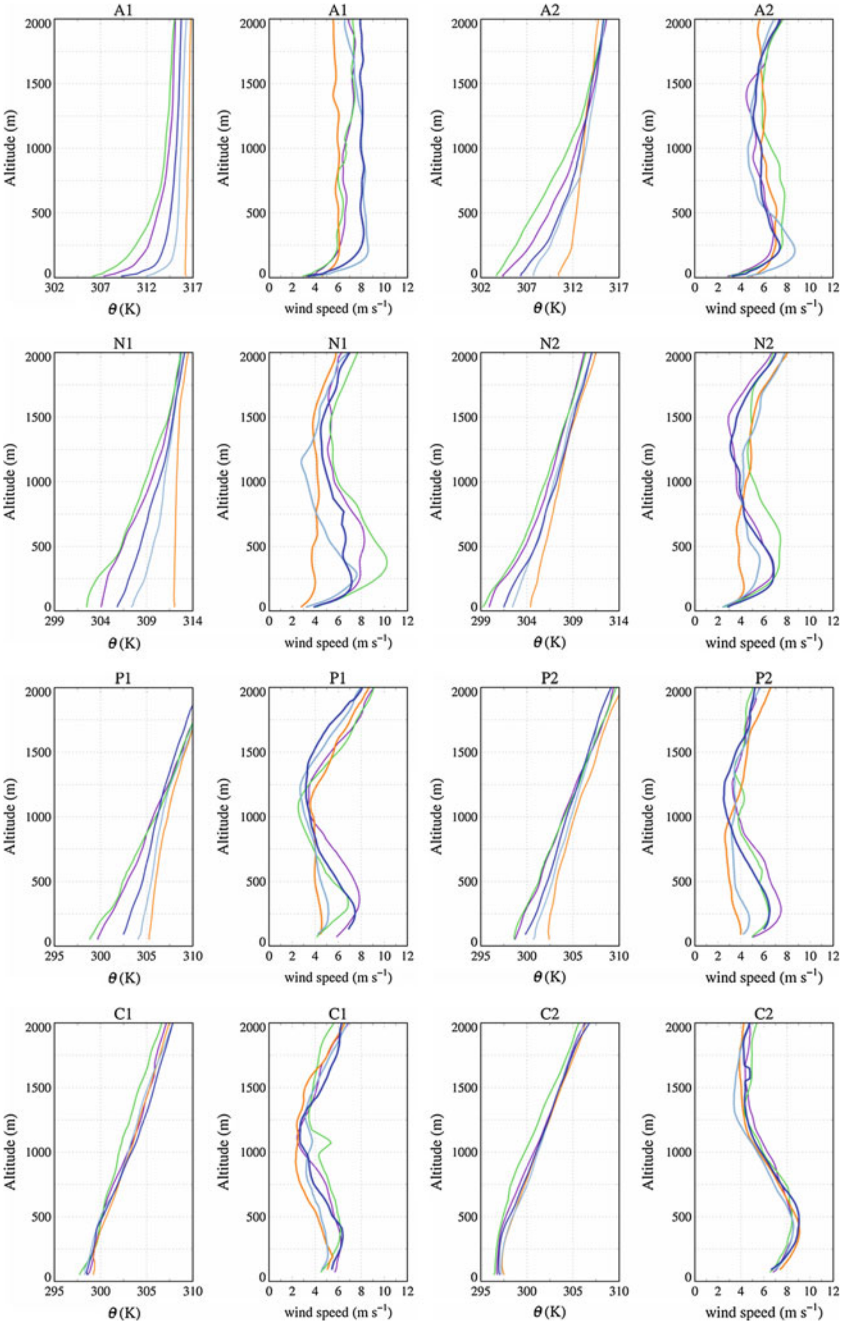

Fig. 13 Mean atmospheric profiles of potential temperature and wind speed made from radiosoundings at Agadez (*top plots*), Niamey (*top middle plots*), Parakou (*bottom middle plots*) and Cotonou (*bottom plots*) during SOP-1 (*left plots*) and SOP-2 (*right plots*) launched at 1800 UTC (*orange*), 2100 UTC (*light blue*), 2400 UTC (*dark blue*), 0300 UTC (*purple*) and 0600 UTC (*green*)

References

Abdou K, Parker DJ, Brooks B, Kalthoff N, Lebel T (2010) The diurnal cycle of lower boundary layer wind in the West African monsoon. Q J R Meteorol Soc 136:66–76

Agusti-Panareda A, Beljaars A, Ahlgrimm M, Balsamo G, Bock O, Forbes R, Ghelli A, Guichard F, Kohler M, Meynadier R, Morcrette JJ (2010) The ECMWF re-analysis for the AMMA observational campaign. Q J R Meteorol Soc 136:1457–1472

Bain CL, Parker DJ, Taylor CM, Kergoat L, Guichard F (2010) Observations of the nocturnal boundary layer associated with the West African Monsoon. Mon Weather Rev 138:3142–3156

Benner TC, Curry JA (1998) Characteristics of small tropical cumulus clouds and their impact on the environment. J Geophys Res 103:28753–28767

Betts AK (2006) Radiative scaling of the nocturnal boundary and the diurnal temperature range. J Geophys Res—Atmospheres 111:D7. doi:10.1029/2005JD006560

Betts AK, Jakob C (2002) Evaluation of the diurnal cycle of precipitation, surface thermodynamics, and surface fluxes in the ECMWF model using LBA data. J Geophys Res—Atmosphere 107(D20):8045. doi:10.1029/2001JD000427

Boone A, de Rosnay P, Basalmo P, Beljaars A, Chopin F, Decharme B, Delire C, Ducharne A, Gascoin S, Grippa M, Guichard F, Gusev Y, Harris P, Jarlan L, Kergoat L, Mougin E, Nasonova O, Norgaard A, Orgeval T, Ottlé C, Poccard-Leclercq I, Polcher J, Sandholt I, Saux-Picart S, Taylor C, Xue Y (2009) The AMMA Land Surface Model Intercomparison Project. Bull Am Meteorol Soc 90(12):1865–1880. doi:10.1175/2009BAMS2786.1

Bouniol D, Couvreux F, Kamsu-Tamo PH, Leplay M, Guichard F, Favot F, O'Connor EJ (2012) Diurnal and seasonal cycles of cloud occurrences, types and radiative impact over West Africa. J Appl Meteorol. doi:10.1175/JAMC-D-11-051.1

Canut G, Lothon M, Saïd F, Lohou F (2010) Observation of entrainment at the interface between monsoonal flow and the saharan air layer. Q J R Meteorol Soc 136:34–46

Charney JG (1975) Dynamics of deserts and drought in the Sahel. Q J R Meteorol Soc 101:193–202

Chou C, Neelin JD (2003) Mechanisms limiting the northward extent of the northern summer monsoons over North America, Asia, and Africa. J Clim 16:406–425

Couvreux F, Rio C, Guichard F, Lothon M, Canut G, Bouniol D, Gounou A (2012) Initiation of daytime local convection in a semi-arid region analysed with high-resolution simulations and AMMA observations. Q J R Meteorol Soc 138:56–71. doi:10.1002/qj.903

Cuesta J, Edouart D, Mimouni M, Flamant P, Loth C, Gibert F, Marnas F, Bouklila A, Kharef M, Ouchène B, Kadi M, Flamant C (2008) Multiplatform observations of the seasonal evolution of the Saharan atmospheric boundary layer in Tamanrasset, Algeria, in the framework of the African Monsoon Multidisciplinary Analysis field campaign conducted in 2006. J Geophys Res 113:D00C07. doi:10.1029/2007JD009417

Dolman AJ, Culf AD, Bessemoulin P (1997) Observations of boundary layer developments during the Hapex–Sahel intensive observation period. J Hydrol 188–189:998–1016

Eltahir EAB, Gong C (1996) Dynamics of wet and dry years in West Africa. J Clim 9:1030–1042

Fink AH, Vincent DG, Ermert V (2006) Rainfall types in the West African Sudanian Zone during the Summer Monsoon 2002. Mon Weather Rev 134:2143–2164

Fleming JR, Cox SK (1974) Radiative effects of cirrus clouds. J Atmos Sci 31:2182–2188

Gounou A (2011) The driving processes behind the diurnal cycles of the West African Monsoon. PhD thesis, Université Paul Sabatier, Toulouse III

Goutorbe JP, Lebel T, Tinga A, Bessemoulin P, Brouwer J, Dolman A, Engman E, Gash J, Hoepffner M, Kabat P, Kerr Y, Monteny B, Prince S, Said F, Sellers P, Wallace J (1994) Hapex-Sahel: a large-scale study of land–atmosphere interactions in the semi-arid tropics. Ann Geophys 12:53–64

Guichard F, Petch C, Redelsperger JL, Bechtold P, Chaboureau JP, Cheinet S, Grabowski W, Grenier H, Jones CG, Köhler M, Piriou JM, Tailleux R, Tomasini M (2004) Modelling the diurnal cycle of deep precipitating convection over land with cloud-resolving models and single-column models. Q J R Meteorol Soc 130:3139–3172

Guichard F, Couvreux F, Nuret M, Agusti-Panareda A (2008) Roles of low-level thermodynamics on surface–convection interactions over West-Africa. In: European Geosciences Union General Assembly, Vienna, Austria, 13–18 April 2008 AS1.14-1TH2O-001

Guichard F, Kergoat L, Mougin E, Timouk F, Baup F, Hiernaux P, Lavenu F (2009) Surface thermodynamics and radiative budget in the Sahelian Gourma: seasonal and diurnal cycles. J Hydrol 375:161–177

Hastenrath S (1995) Climate dynamics of the tropics. Kluwer, New York, 488 pp

Hourdin F, Musat I, Guichard F, Ruti PM, Favot F, Filiberti MA, Pham M, Grandpeix JY, Polcher J, Marquet P, Boone A, Lafore JP, Redelsperger JL, Dell'Aquila A, Doval TL, Traore AK, Gallée H (2010) AMMA-Model Intercomparison Project. Bull Am Meteorol Soc 91(1):95–104

Janicot S, Thorncroft CD, Ali A, Asencio N, Berry G, Bock O, Bourles B, Caniaux G, Chauvin F, Deme A, Kergoat L, Lafore JP, Lavaysse C, Lebel T, Marticorena B, Mounier F, Nedelec P, Redelsperger JL, Ravegnanni F, Reeves CE, Roca R, De Rosnay P, Schlager H, Sultan B, Tomasini M, Ulanovsky A (2008) Large-scale overview of the summer monsoon over West Africa during the AMMA field experiment in 2006. Ann Geophys 26:2569–2595

Karbou F, Gérard E, Rabier F (2010) Global 4DVAR assimilation and forecast experiments using AMSU Observations over Land. Part I: impacts of various land surface emissivity parameterizations. Wea Forecast 25:5–19. doi:10.1175/2009WAF2222243.1

Kocha C, Lafore JP, Tulet P, Seiti Y (2012) High resolution simulation of major West African storm: comparison with observations and investigation of dust impacts. Q J R Meteorol Soc. doi:10.1002/qj.927

Kohler M, Kalthoff N, Kottmeier C (2010) The impact of soil moisture modifications on cbl characteristics in west Africa: a case-study from the AMMA campaign. Q J R Meteorol Soc 136:442–455

Lebel T, Diedhiou A, Laurent H (2003) Seasonal cycle and interannual variability of the Sahelian rainfall at hydrological scales. J Geophys Res 108(D8):8389. doi:10.1029/2001JD001580

Lebel T, Parker DJ, Flamant C, Bourles B, Marticorena B, Mougin E, Peugeot C, Diedhiou A, Haywood JM, Ngamini JB, Polcher J, Redelsperger JL, Thorncroft CD (2010) The AMMA field campaigns: multiscale and multidisciplinary observations in the West African region. Q J R Meteorol Soc 136:8–33

Lothon M, Said F, Lohou F, Campistron B (2008) Observation of the diurnal cycle in the low troposphere of West Africa. Mon Weather Rev 136:3477–3500

Lothon M, Campistron B, Chong M, Couvreux F, Guichard F, Rio C, Williams E (2011) Life cycle of a mesoscale circular gust front observed by a C-Band Doppler Radar in West Africa. Mon Weather Rev 139:1370–1388

Love T, Kumar V, Xie P, Thiaw WM (2004) 20-year daily Africa precipitation climatology using satellite and gauge data. In: Proceedings of 84th AMS annual meeting. American Meteorological Society, Seattle, WA P5.4 (CD-ROM)

Marht (1991) Boundary-layer moisture regimes. Q J R Meteorol Soc 117:151–176

Mathon V, Laurent H, Lebel T (2002) Mesoscale convective system rainfall in the Sahel. J Appl Meteorol 41:1081–1092

McAvaney B, Le Treut H (2003) The Cloud Feedback Intercomparison Project: CFMIP. In: CLIVAR Exchanges—supplementary contributions. 26 March

Miller MA, Slingo A (2007) The ARM mobile facility and its first international deployment. Bull Am Meteorol Soc 1229-1244

Mougin E, Hiernaux P, Kergoat L, Grippa M, de Rosnay P, Timouk F, Le Dantec V, Demarez V, Lavenu F, Arjounin M, Lebel T, Soumaguel N, Ceschia E, Mougenot B, Baup F, Frappart F, Frison PL, Gardelle J, Gruhier C, Jarlan L, Mangiarotti S, Sanou B, Tracol Y, Guichard F, Trichon V, Diarra L, Soumaré A, Koité M, Dembélé F, Lloyd C, Hanan NP, Damesin C, Delon C, Serça D, Galy-Lacaux C, Seghieri J, Becerra S, Dia H, Gangneron F, Mazzega P (2009) The AMMA-CATCH Gourma observatory site in Mali: relating climatic variations to changes in vegetation, surface hydrology, fluxes and natural resources. J Hydrol 375:14–33

Nicholson S (1980) The nature of rainfall fluctuations in subtropical West Africa. Mon Weather Rev 108:473–487

Nicholson S, Grist JP (2003) The seasonal evolution of the atmospheric circulation over West Africa and equatorial Africa. J Clim 16:1013–1030

Nuret M, Lafore JP, Guichard F, Redelsperger JL, Bock O, Agusti-Panareda A, N'Gamini JB (2008) Correction of humidity bias for Vaisala RS80-A Sondes during the AMMA 2006 observing period. J Atmos Oceanic Technol 25:2152–2158. doi:10.1175/2008JTECHA1103.1

Parker DJ, Burton RR, Diongue-Niang A, Ellis RJ, Felton M, Taylor CM, Thorncroft CD, Bessemoulin P, Tompkins AM (2005) The diurnal cycle of the West African monsoon circulation. Q J R Meteorol Soc 131:2839–2860

Parker DJ, Fink A, Janicot S, Ngamini JB, Douglas M, Afiesimama E, Agusti-Panareda A, Beljaars A, Dide F, Diedhiou A, Lebel T, Polcher J, Redelsperger JL, Thorncroft C, Wilson GA (2008) The AMMA radiosonde program and its implications for the future of atmospheric monitoring over Africa. Bull Am Meteorol Soc 89:1015–1027

Peyrillé P, Lafore JP (2007) An idealized two-dimensional framework to study the West African Monsoon. Part II: large-scale advection and the diurnal cycle. J Atmos Sci 64:2783–2803

Ramier D, Boulain N, Cappelaere B, Timouk F, Rabanit M, Lloyd CR, Boubkraoui S, Métayer F, Descroix L, Wawrzyniak V (2009) Towards an understanding of coupled physical and biological processes in the cultivated Sahel −1. Energy and water. J Hydrol 375(1–2):204–216

Redelsperger JL, Thorncroft C, Diedhiou A, Lebel T, Parker DJ, Polcher J (2006) African Monsoon Multidisciplinary Analysis (AMMA): an international research project and field campaign. Bull Am Meteorol Soc 87:1739–1746

Samain O, Kergoat L, Hiernaux P, Guichard F, Mougin E, Timouk F, Lavenu F (2008) Analysis of the in-situ and MODIS albedo variability at multiple time scales in the Sahel. J Geophys Res 113:D14119. doi:10.1029/2007JD009174

Söhne N, Chaboureau JP, Guichard F (2008) Verification of cloud cover forecast with satellite observation over West Africa. Mon Weather Rev 136:4421–4434. doi:10.1175/2008MWR2432.1

Stein THM, Parker DJ, Delanoë J, Dixon NS, Hogan RJ, Knippertz P, Maidment RI, Marsham JH (2011) The vertical cloud structure of the West African monsoon: a 4 year climatology using CloudSat and CALIPSO. J Geophys Res 116:D22205. doi:10.1029/2011JD016029

Stull RB (1988) An introduction to boundary layer meteorology. Kluwer, Dordrecht, 666 pp

Sultan B, Janicot S (2003) The West African monsoon dynamics. Part II: the “preonset” and “onset” of the summer monsoon. J Clim 16:3407–3427

Svensson G, Holtslag AAM, Kumar V, Mauritsen T, Steeneveld GJ, Angevine WM, Bazile E, Beljaars A, de Bruijn EIF, Cheng A, Conangla L, Cuxart J, Ek M, Falk MJ, Freedman F, Kitagawa H, Larson VE, Lock A, Mailhot J, Masson V, Park S, Pleim J, Söderberg S, Weng W, Zampieri M (2011) Evaluation of the diurnal cycle in the atmospheric boundary layer over land as represented by a variety of single-column models: the second GABLS experiment. Boundary-Layer Meteorol 140:177–206. doi:10.1007/s10546-011-9611-7

Thorncroft C, Parker DJ, Burtoon RR, Diop M, Ayers JH, Barjat H, Devereau S, Diongue A, Dumelow R, Kindred DR, Price NM, Saloum M, Taylor CM, Tompkins AM (2003) The JET2000 Project: aircraft observations of the African easterly jet and African easterly waves. Bull Am Meteorol Soc 84:337–357

Timouk F, Kergoat L, Mougin E, Lloyd CR, Ceschia E, Cohard JM, de Rosnay P, Hiernaux P, Demarez V, Taylor CM (2009) Response of surface energy balance to water regime and vegetation development in a Sahelian landscape. J Hydrol 375(1–2):178–189

van Heerwaarden CC, Vila-Guerau de Arellano J, Gounou A, Guichard F, Couvreux F (2010) Understanding the daily cycle of surface evapotranspiration: a new method to quantify the influence of forcings and feedbacks. J Hydromet. doi:10.1175/2010JHM1272.1

Wai MMK, Smith EA, Bessemoulin P, Culf AD, Dolman AJ, Lebel T (1997) Variability in boundary layer structure during Hapex-Sahel wet-dry season transition. J Hydrol 188–189:965–997

White F (1983) The vegetation of Africa. UNESCO, Paris, 356 pp

Williams KD, Ringer MA, Senior CA, Webb MJ, Mc Avaney B, Andronova N, Bony S, Dufresne JL, Emori S, Gudgel R, Knutson T, Li B, Lo K, Musat I, Wegner J, Slingo A, Mitchell JFB (2006) Evaluation of a component of the cloud response to climate change in an intercomparison of climate models. Clim Dyn 26:145–165. doi:10.1007/s00382-005-0067-7

Yang CY, Slingo J (2001) The diurnal cycle in the tropics. Mon Weather Rev 129:784–801